NOTES AND CORRESPONDENCE

On the Dynamics of β Plumes

TAMAY M. ÖZGÖKMEN

RSMAS, University of Miami, Miami, Florida

FULVIO CRISCIANI

CNR, Istituto Talassografico di Trieste, Trieste, Italy

27 October 2000 and 8 June 2001

ABSTRACT

The dynamics of zonal recirculating flows (β plumes) driven by a source of potential vorticity, or a sink of mass, located at the eastern boundary of an ocean basin are investigated using analytical solutions of the barotropic, linear, steady quasigeostrophic equation with bottom and lateral friction.

By scaling the ratio of the strength of the recirculation to that of the sink by that from the inviscid solution, the regimes are identified in which friction becomes a dominant factor. The primary new finding of this study is that the recirculating flow component disappears due to frictional effects when the meridional extent of the sink becomes small. Unlike for the zonal extent of the sink, which affects the recirculating component only if it is on the order of the frictional boundary layer scale, the deviation of the recirculating flow strength from that given by the inviscid solution is apparent for meridional sink scales, which are much larger than the frictional boundary layer scale. Also, location of the maximum recirculation and westward penetration distance of the plumes are quantified. Finally, a stability analysis is conducted to determine the parameter regime in which the β plumes are candidates for instability.

1. Introduction

Recent studies using primitive equation (Jia 2000) and quasigeostrophic (Özgökmen et al. 2001) general circulation models indicate that entrainment of overlying Atlantic water into descending dense Mediterranean overflow exiting the Strait of Gibraltar may be responsible for the formation of the Azores Current (Käse and Siedler 1982; Gould 1985; Käse et al. 1985; Klein and Siedler 1989; Käse and Krauss 1996). Özgökmen et al. (2001) idealized the loss of fluid from the upper ocean as a source of potential vorticity. The adequacy of this formulation was justified by a comparison of quasigeostrophic simulations with results from a primitive equation model (the Miami Isopycnic Coordinate Ocean Model), in which divergent flow effects associated with entrainment were explicitly represented. A localized loss of mass from the active layer generates a cyclonic eddy that elongates westward under the influence of the β effect. In the steady state, the circulation pattern induced by such a process consists of bidirectional zonal flows: eastward to the south of the sink and westward to the north, as described by Pedlosky (1996).

The mechanism highlighted by Özgökmen et al. (2001) to explain the existence of the Azores Current therefore relies on the so-called β plume, originally proposed by Stommel (1982) as a reason for the westward extended chemical signature in the Pacific Ocean. The primary new contribution has been recognition that when a localized sink of scale O(100 km) and of strength $O(1\ \text{Sv} \equiv 10^6\ \text{m}^3\ \text{s}^{-1})$ [consistent with observations of the Mediterranean overflow process (Baringer and Price 1997a,b)] is placed near the eastern boundary of a midlatitude circulation, it alters significantly the wind-driven upper ocean flow and induces an eastward zonal current, which resembles the Azores Current in location and transport. The β-plume mechanism necessarily generates also a westward current, which may be associated with the so-called Azores Countercurrent, the existence of which is supported by various observational studies (Onken 1993; Cromwell et al. 1996; Iorga and Lozier 1999a,b). Using hydrographic data, Mauritzen et al. (2001) show cyclonic circulation in the Gulf of Cadiz, which maybe interpreted as the source of the Azores

Corresponding author address: Dr. Tamay M. Özgökmen, RSMAS/MPO, University of Miami, 4600 Rickenbacker Causeway, Miami, FL 33149-1098.
E-mail: tozgokmen@rsmas.miami.edu

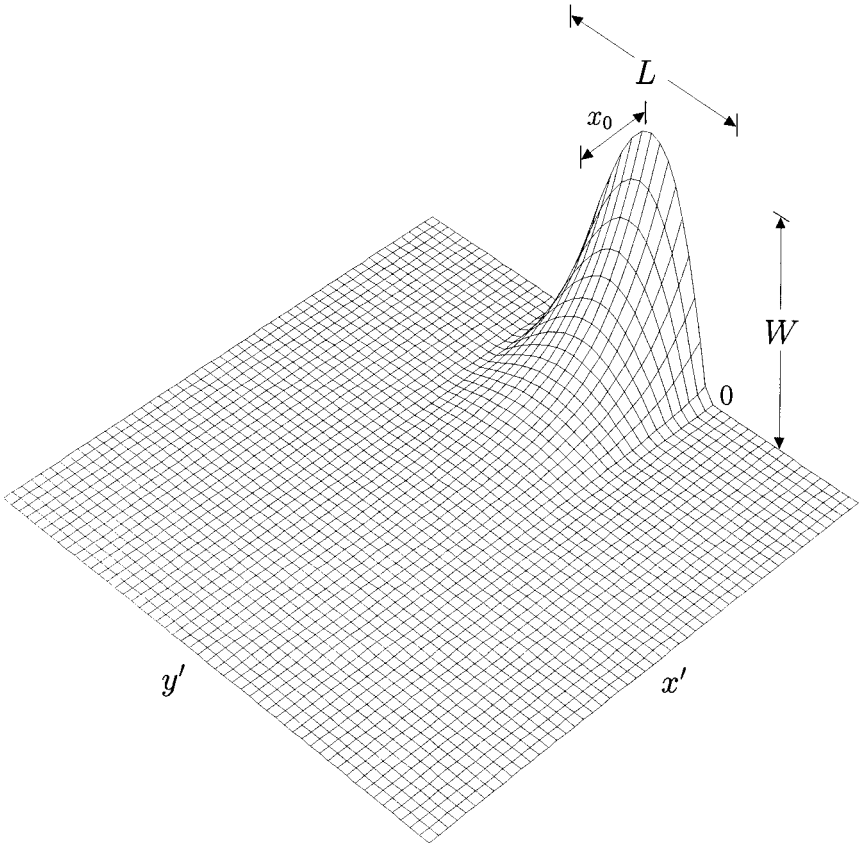

FIG. 1. Schematic illustration of sink distribution $w'(x', y')$.

Countercurrent, and is an essential feature for the β-plume mechanism to be valid.

Since the forcing associated with this β plume is near or at the eastern boundary of the basin, it is of interest to investigate the effect of frictional processes on the strength of the induced recirculation. Spall (2000) recognized that frictional terms can become of leading order in the potential vorticity budget when such regions of localized forcing are adjacent to a boundary. Consequently, recirculating flows may diminish when the forcing is within the frictional boundary layer and only the unidirectional flow into (or out of) the region remains. This unidirectional flow component is that which compensates for the mass loss/gain. The inviscid theory (Pedlosky 1996; Spall 2000) gives the ratio of the recirculating flow to that of sink as $f_0/\beta L$, where f_0 is the Coriolis frequency, β the meridional gradient of planetary vorticity, and L the meridional scale of the sink. This ratio, $f_0/\beta L \gg 1$ at midlatitudes and for small-scale sinks, such that the recirculating flow component is much stronger than that compensating for the mass loss/gain. Spall's (2000) analytical solutions are in agreement with primitive equation model results. However, the one-dimensional (zonal) nature of these analytical solutions precludes any conclusions in regard to the behavior of β plumes when their meridional scale is decreased, which is of particular interest considering that the entrainment in the Mediterranean overflow takes place over a distance on the order of 100 km (Baringer and Price 1997b), hence in a very localized manner.

In the present study, we focus on determining the ratio of recirculating and sinking transports of β plumes as a function of two important physical parameters, the meridional scale of the sink and the friction coefficient, using two-dimensional analytical solutions of a steady, linear, barotropic, quasigeostrophic model in which the sink is placed at the eastern boundary of an ocean basin. The present study, involving two-dimensional solutions and focusing on the impact of friction on sinks at various meridional scales, is a natural extension of the corresponding section in the study by Spall (2000).

The paper is organized as follows: In section 2, linear solutions of quasigeostrophic β plumes with bottom and lateral dissipation are presented. The properties of these solutions are discussed in section 3, with particular emphasis on the ratio of the recirculating flow to that of sink. A stability analysis is carried out in section 4. Finally, the results are summarized in section 5, and recommendations for future studies are outlined.

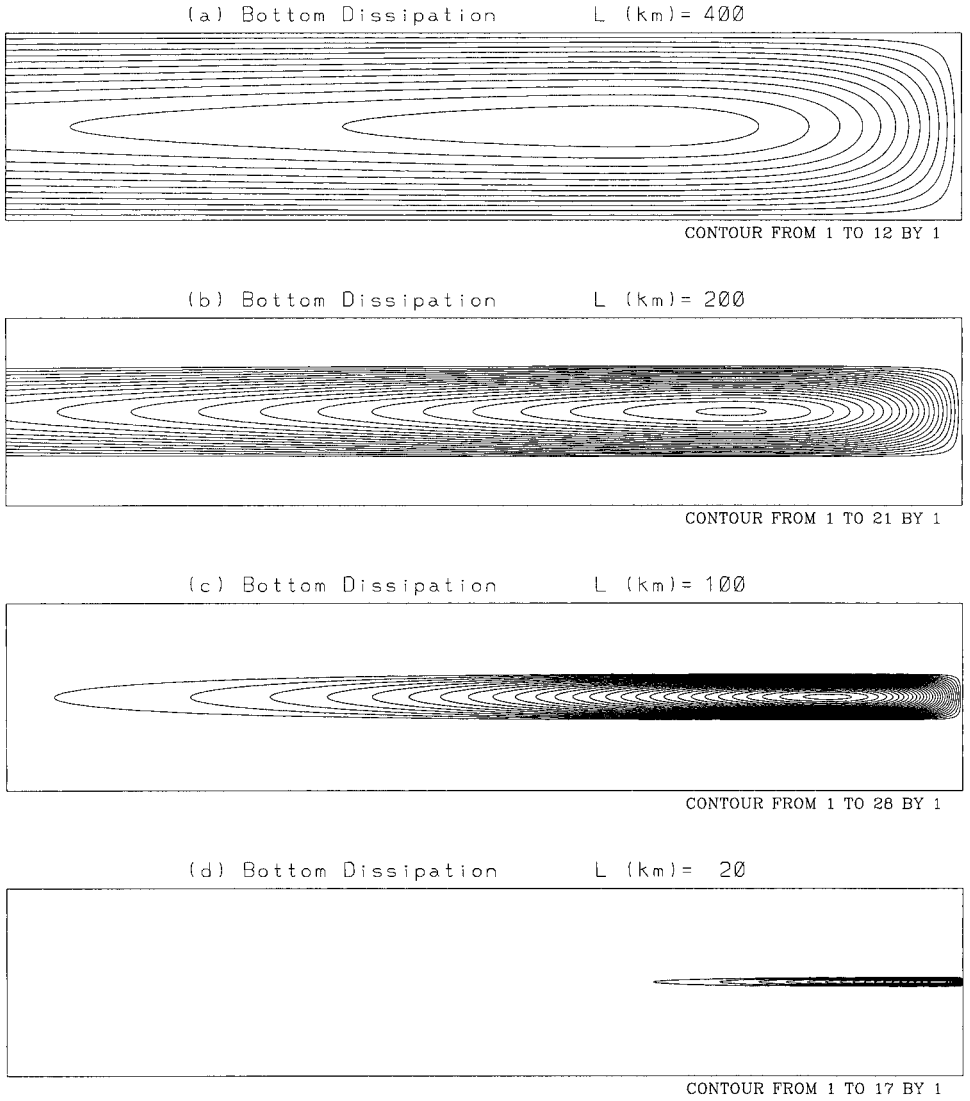

FIG. 2. Contours of the ratio of transport streamfunction $\psi' H$ and total sink transport (contour interval: 1) with bottom dissipation in a domain with dimensions of 2000 km × 400 km in zonal and meridional directions, respectively. Other parameters are $\theta_0 = 30°\text{N}$ ($\beta = 2 \times 10^{-11}$ m^{-1} s^{-1}), $r = 5 \times 10^{-8}$ s^{-1} ($\delta = 2.5$ km), $x_0 = 200$ km ($d = 80$). (a) $L = 400$ km ($l = 160$), (b) $L = 200$ km ($l = 80$), (c) $L = 100$ km ($l = 40$), and (d) $L = 20$ km ($l = 8$).

2. Solutions for quasigeostrophic linear β plumes

We seek solutions to the equivalent-barotropic, steady, linear, quasigeostrophic equation, in which entrainment is represented by potential vorticity forcing:

$$\beta \frac{\partial \psi'}{\partial x'} = \frac{f_0}{H} w' + D, \tag{1}$$

where primes denote dimensional variables, $\psi'(x', y')$ is the streamfunction, f_0 the Coriolis frequency at a reference latitude, β the meridional gradient of the planetary vorticity, and H the depth of motion. The fluid domain is $(-\infty < x' \leq 0) \times (-\infty < y' < +\infty)$ where $x' = 0$ is the longitude of the eastern coast. The entrainment term is nonvanishing only over a zonal strip and decays exponentially as follows:

$$w'(x', y') = W \exp\left(\frac{x'}{x_0}\right) \sin\left(\pi \frac{y'}{L}\right) \quad \text{and}$$

$$w'(x', y') = 0, \quad \text{for } y' < 0 \quad \text{and} \quad y' > L, \tag{2}$$

where $W = w'(0, L/2)$, L is the meridional extent, and x_0 the zonal e-folding scale of the forcing (Fig. 1). The dissipation takes place either via bottom or lateral friction:

$$D = \begin{cases} -r\nabla^2\psi' & \text{for bottom friction} \\ +\nu\nabla^4\psi' & \text{for lateral friction,} \end{cases} \tag{3}$$

where r and ν are the bottom and lateral friction coefficients, respectively, and $\nabla^2 = \partial^2/\partial x'^2 + \partial^2/\partial y'^2$ is the Laplacian.

The primary difference of the above system of equations from those in Spall (2000) is that the above system is two-dimensional as opposed to one-dimensional, and we consider a continuously distributed forcing function as opposed to a discontinuous one (i.e., step function). However, the derivative in the y' direction of the forcing is discontinuous at $y' = 0$ and $y' = L$.

a. Solution for bottom dissipation case

Introducing the following nondimensional variables,

$$(x', y') = L(x, y); \qquad \psi' = \frac{f_0 WL}{\beta H}\psi; \qquad w' = Ww, \quad (4)$$

and substituting into (1), the nondimensional governing equation for the bottom dissipation case becomes

$$\frac{\partial \psi}{\partial x} = \exp\left(\frac{L}{x_0}x\right)\sin(\pi y) - \frac{\delta_s}{L}\nabla^2\psi, \quad (5)$$

where $\delta_s = r/\beta$ is the boundary layer scale due to bottom friction.

Using separation of variables

$$\psi(x, y) = \phi(x)\sin(\pi y) \quad (6)$$

and the homogeneous equation $\psi_x = -L^{-1}\delta_s\nabla^2\psi$, the equation for ϕ becomes

$$\frac{d^2\phi}{dx^2} + \frac{L}{\delta_s}\frac{d\phi}{dx} - \pi^2\phi = 0, \quad (7)$$

subject to the boundary conditions

$$\phi(-\infty) = 0 \quad \text{and} \quad \phi(0) = 0. \quad (8)$$

Note that (8) is equivalent to imposing no net meridional flow. The solution to (7), (8) is (e.g., Spiegel 1991)

$$\phi(x) = \exp\left[\left(-\frac{L}{2\delta_s} + \sqrt{\left(\frac{L}{2\delta_x}\right)^2 + \pi^2}\right)x\right]. \quad (9)$$

To solve for the inhomogeneous case, we set $\psi = Aw$ and substitute into (5) to find the amplitude A, and get

$$\psi = \left[\frac{L}{x_0} + \frac{\delta_s L}{x_0^2} - \frac{\delta_s}{L}\pi^2\right]^{-1} w. \quad (10)$$

Note that because of (2), (10) implies $\psi(-\infty, y) = 0$.

The total solution for the bottom dissipation case becomes

$$\psi(x, y) = \left[\frac{L}{x_0} + \frac{\delta_s L}{x_0^2} - \frac{\delta_s}{L}\pi^2\right]^{-1}\left\{\exp\left(\frac{L}{x_0}x\right) - \exp\left[\left(-\frac{L}{2\delta_s} + \sqrt{\left(\frac{L}{2\delta_s}\right)^2 + \pi^2}\right)x\right]\right\}\sin(\pi y). \quad (11)$$

Introducing

$$l = \frac{L}{\delta_s} \quad \text{and} \quad d = \frac{x_0}{\delta_s} \quad (12)$$

as the ratios of meridional and zonal scales of the sink to the frictional boundary layer scale, respectively, (11) is rewritten as

$$\psi(x, y) = \frac{d^2 l}{dl^2 + l^2 - d^2\pi^2}\left\{\exp\left(\frac{l}{d}x\right) - \exp\left[\left(-\frac{d}{2} + \sqrt{\left(\frac{d}{2}\right)^2 + \left(\frac{\pi d}{l}\right)^2}\right)\frac{l}{d}x\right]\right\}\sin(\pi y). \quad (13)$$

b. Solutions for lateral dissipation case

In this case, the nondimensional governing equation is

$$\frac{\partial \psi}{\partial x} = \exp\left(\frac{L}{x_0}x\right)\sin(\pi y) + \left(\frac{\delta_M}{L}\right)^3\nabla^4\psi, \quad (14)$$

where $\delta_M = (\nu/\beta)^{1/3}$ is the boundary layer scale due to lateral friction. Using $\psi(x, y) = \phi(x)\sin(\pi y)$, the equation for ϕ becomes

$$\frac{d\phi}{dx} = \exp\left(\frac{L}{x_0}x\right) + \left(\frac{\delta_M}{L}\right)^3\left(\frac{d^4\phi}{dx^4} - 2\pi^2\frac{d^2\phi}{dx^2} + \pi^4\phi\right). \quad (15)$$

A special solution satisfying (15) is $\tilde{\phi} = A\exp(L/x_0 x)$, and substituting in to find the amplitude A, we obtain

$$\tilde{\phi} = \left[\frac{L}{x_0} - \left(\frac{\delta_M}{L}\right)^3\left(\frac{L^4}{x_0^4} - 2\pi^2\frac{L^2}{x_0^2} + \pi^4\right)\right]^{-1}\exp\left(\frac{L}{x_0}x\right). \quad (16)$$

The general integral of the homogeneous form of (15)

is the superposition of terms of the kind $\exp(\lambda x)$, where the algebraic equation for λ can be written as

$$\lambda = \left(\frac{\delta_M}{L}\right)^3 (\lambda^2 - \pi^2)^2. \tag{17}$$

Defining $F(\lambda) = [\lambda^2 - \pi^2]^2$ and expanding around π up to second order in λ, $F(\lambda) \approx 4\pi^2(\lambda - \pi)^2$, and Eq. (17) is approximated by

$$\lambda = \left(\frac{\delta_M}{L}\right)^3 4\pi^2(\lambda - \pi)^2. \tag{18}$$

Setting

$$\epsilon = \left(\frac{L}{\delta_M}\right)^3 \frac{1}{4\pi^2}, \tag{19}$$

we obtain

$$\lambda_\pm = \pi + \frac{\epsilon}{2} \pm \sqrt{\pi\epsilon + \left(\frac{\epsilon}{2}\right)^2}. \tag{20}$$

Note that

$$\pi\epsilon + \left(\frac{\epsilon}{2}\right)^2 = \left(\pi + \frac{\epsilon}{2}\right)^2 - \pi^2 < \left(\pi + \frac{\epsilon}{2}\right)^2,$$

so both roots λ_+ and λ_- are positive.

Defining for convenience

$$N_L = \left[\frac{L}{x_0} - \left(\frac{\delta_M}{L}\right)^3 \left(\frac{L^4}{x_0^4} - 2\pi^2\frac{L^2}{x_0^2} + \pi^4\right)\right]^{-1}, \tag{21}$$

the total solution for ϕ can be written as

$$\phi = N_L \exp\left(\frac{L}{x_0}x\right) + C_1 \exp(\lambda_+ x) + C_2 \exp(\lambda_- x). \tag{22}$$

No mass-flux boundary condition at the eastern boundary $x = 0$ demands that

$$N_L + C_1 + C_2 = 0. \tag{23}$$

At this point, boundary conditions in addition to no mass flux are needed to solve for C_1 and C_2. We consider the following no-slip boundary condition. (The solution for free-slip boundary condition is straightforward, and it is not shown here.)

Imposing $[d\phi/dx]_{x=0} = 0$, we find from (22)

$$N_L\frac{L}{x_0} + C_1\lambda_+ + C_2\lambda_- = 0. \tag{24}$$

From (23) and (24) we solve for C_1 and C_2 to find the expression of ϕ, and the total solution for ψ becomes

$$\psi(x, y) = \left[\frac{L}{x_0} - \left(\frac{\delta_M}{L}\right)^3 \left(\frac{L^4}{x_0^4} - 2\pi^2\frac{L^2}{x_0^2} + \pi^4\right)\right]^{-1} \left[\exp\left(\frac{L}{x_0}x\right) + \frac{\lambda_- - \frac{L}{x_0}}{\lambda_+ - \lambda_-}\exp(\lambda_+ x) - \frac{\lambda_+ - \frac{L}{x_0}}{\lambda_+ - \lambda_-}\exp(\lambda_- x)\right] \sin(\pi y). \tag{25}$$

Introducing

$$l^* = \frac{L}{\delta_M} \quad \text{and} \quad d^* = \frac{x_0}{\delta_M} \tag{26}$$

as the ratios of meridional and zonal scales of the sink to the frictional boundary layer scale, respectively, (25) is rewritten as

$$\psi(x, y) = \frac{l^{*3}d^{*4}}{l^{*4}d^{*3} - l^{*4} + 2\pi^2 l^{*2}d^{*2} - \pi^4 d^{*4}}\left[\exp\left(\frac{l^*}{d^*}x\right) + \frac{\lambda_- - \frac{l^*}{d^*}}{\lambda_+ - \lambda_-}\exp(\lambda_+ x) - \frac{\lambda_+ - \frac{l^*}{d^*}}{\lambda_+ - \lambda_-}\exp(\lambda_- x)\right] \sin(\pi y). \tag{27}$$

However, solution (27) does not work when

$$\left(\frac{L^2}{x_0^2} - \pi^2\right)^2 = \left(\frac{L}{\delta_M}\right)^3 \frac{L}{x_0}, \tag{28}$$

since this is where N_L has a pole. In order to find the solution at this pole, we seek for a solution of the kind

$$\phi(x) = Nx \exp\left(\frac{L}{x_0}x\right). \tag{29}$$

Substitution of (29) into (15) yields

$$N\left(4\frac{L^3}{x_0^3} + x\frac{L^4}{x_0^4}\right) - 2\pi^2 N\left(2\frac{L}{x_0} + x\frac{L^2}{x_0^2}\right)$$

$$-\left(\frac{L}{\delta_M}\right)^3 N\left(1 + x\frac{L}{x_0}\right) + Nx\pi^4 = -\left(\frac{L}{\delta_M}\right)^3. \quad (30)$$

Hence

$$N\left[4\frac{L^3}{x_0^3} - 4\pi^2\frac{L}{x_0} - \left(\frac{L}{\delta_M}\right)^3\right] = -\left(\frac{L}{\delta_M}\right)^3 \quad \text{and} \quad (31)$$

$$N\left[\frac{L^4}{x_0^4} - 2\pi^2\frac{L^2}{x_0^2} - \left(\frac{L}{\delta_M}\right)^3\frac{L}{x_0} + \pi^4\right] = 0. \quad (32)$$

From (31)

$$N = \frac{\left(\frac{L}{\delta_M}\right)^3}{\left(\frac{L}{\delta_M}\right)^3 + 4\pi^2\frac{L}{x_0} - 4\left(\frac{L}{x_0}\right)^3}, \quad (33)$$

while (32) implies

$$\left(\frac{L^2}{x_0^2} - \pi^2\right)^2 = \left(\frac{L}{\delta_M}\right)^3\frac{L}{x_0},$$

which is identically satisfied by (28). Therefore, the solution at the pole can be written as

$$\phi = Nx\exp\left(\frac{L}{x_0}x\right) + D_1\exp(\lambda_+ x) + D_2\exp(\lambda_- x), \quad (34)$$

where N is given by (33). Applying $\phi(0) = 0$, no flow, and $[d\phi/dx]_{x=0} = 0$, no-slip conditions to find the constants D_1 and D_2, the total solution in (d^*, l^*)-space becomes

$$\psi(x, y) = \frac{l^{*3}d^{*3}}{l^{*3}d^{*3} + 4\pi^2 l^* d^{*2} - 4l^{*3}} \times \left[x\exp\left(\frac{l^*}{d^*}x\right) + \frac{\exp(\lambda_- x) - \exp(\lambda_+ x)}{\lambda_+ - \lambda_-}\right] \times \sin(\pi y), \quad (35)$$

which is valid at the pole given by (28).

3. Properties of solutions

a. Circulation patterns

Typical circulation patterns corresponding to β plumes are illustrated in Fig. 2. In these solutions, the domain shown has dimensions of 2000 km × 400 km in the zonal and meridional directions, respectively. The sink is located at 30°N ($\beta = 2 \times 10^{-11}$ m^{-1} s^{-1}) and has a zonal e-folding scale of $x_0 = 200$ km. The bottom friction parameter is $r = 5 \times 10^{-8}$ s^{-1}. Therefore, the frictional boundary layer scale $\delta = 2.5$ km, and the nondimensional parameter $d = 80$. Since $d \gg 1$, the gyres are not affected by friction due to the eastern boundary, based on the results by Spall (2000). The total sink transport is kept constant. Contours of the ratio of transport streamfunction $\psi' H$ and total sink transport are shown as a function of the meridional extent L (or nondimensional parameter l). All solutions (Figs. 2a–d) exhibit the same qualitative behavior: an anticyclonic (cyclonic) recirculation for $W > 0$ ($W < 0$) or a bidirectional flow pattern (westward in the south and eastward in the north for $W > 0$ or opposite for $W < 0$), with a meridional extent of L, as discussed in detail in previous studies (e.g., Pedlosky 1996; Spall 2000). In Fig. 2, both branches carry the same transport due to the neglect of the divergent component by defining a streamfunction in the quasigeostrophic formalism. In agreement with previous work, the ratio of the maximum recirculating transport to the total sink transport initially increases with decreasing L: 12, 21, and 28 for $L = 400$ km, 200 km, and 100 km ($l = 160$, 80, and 40), respectively (Fig. 2a–c), indicating generation of horizontal circulation with a strength $O(10)$ higher than that of the sink. The result of interest appears when the meridional extent of the forcing is reduced. Furthermore, the ratio of the maximum recirculating transport to the total sink transport decreases to 17 for $L = 20$ km ($l = 8$) as shown in Fig. 2d. Therefore, there appears to be a regime when the strength of the recirculation is damped by frictional processes. Similar behavior applies to the lateral friction case as well.

b. Relative strengths of recirculation and upwelling

The behavior of the solutions in a wide parameter space is explored with emphasis on the ratio of the strengths of horizontal recirculation to that of upwelling (sinking). To this end, we define the transport due to upwelling, S, as follows:

$$S \equiv \int_{-\infty}^{+\infty}\int_{-\infty}^{0} w'(x', y')\, dx'\, dy', \quad (36)$$

and using the dimensional upwelling function (2),

$$S = \frac{2}{\pi}Wx_0L. \quad (37)$$

The solution for the bottom dissipation case (13) can be rewritten as

$$\psi' = \frac{f_0 WL}{\beta H}\frac{d}{l}\frac{d}{(1 + d + B)}\frac{1}{(1 - B)} \times \left\{\exp\left(\frac{l}{d}x\right) - \exp\left(B\frac{l}{d}x\right)\right\}\sin(\pi y), \quad (38)$$

where

$$B = \sqrt{\left(\frac{d}{2}\right)^2 + \left(\frac{\pi d}{l}\right)^2} - \frac{d}{2} \quad (39)$$

is defined, for convenience, as a nonlinear combination

of l and d. The maximum transport of the recirculation gyre is

$$R \equiv \psi'(x = x_{\max}, y = 1/2)H, \tag{40}$$

where $x_{\max}$ is the zonal distance from the eastern boundary, at which the strength of the recirculation is maximum. To find $x_{\max}$,

$$\frac{d}{dx}\left[\psi'\left(x, \frac{1}{2}\right)\right] = 0$$

yields

$$x_{\max} = \frac{d}{l}\frac{\ln B}{1 - B}. \tag{41}$$

From (40), (38), and (41), we obtain

$$R = \frac{f_0 WL}{\beta}\frac{d}{l}\frac{d}{(1 + d + B)}\frac{1}{(1 - B)} \times \left\{\exp\left(\frac{\ln B}{1 - B}\right) - \exp\left(B\frac{\ln B}{1 - B}\right)\right\}. \tag{42}$$

From (37) and (42), the ratio of the transports of maximum recirculation to upwelling is then given by

$$\frac{R}{S} = \frac{\pi}{2}\frac{f_0}{\beta L}\frac{d}{(1 + d + B)}\frac{1}{(1 - B)} \times \left\{\exp\left(\frac{\ln B}{1 - B}\right) - \exp\left(B\frac{\ln B}{1 - B}\right)\right\}. \tag{43}$$

The behavior of R/S is first discussed as a function of dimensional physical parameters, and then generalized using nondimensional parameters. The dependence of R/S on two important physical parameters, the meridional scale of upwelling, L, and the friction coefficient, r, is shown in Fig. 3 for a sink located at 30°N and with a zonal e-folding scale of $x_0 = 200$ km (same as in Fig. 2). The parameter range covered in Fig. 3 is $0 \le L \le 2000$ km and $5 \times 10^{-8}\ \text{s}^{-1} \le r \le 5 \times 10^{-4}\ \text{s}^{-1}$ (or as plotted $2 \times 10^3\ \text{s} \le r^{-1} \le 2 \times 10^7$ s). This figure indicates that when the friction coefficient is high (left-hand side of Fig. 3), R/S has small values, which is quite intuitive. The ratio R/S increases as the friction coefficient is reduced (right-hand portion of Fig. 3) and becomes asymptotically independent of the friction coefficient. In this regime (right-hand portion or right vertical axis of Fig. 3), two different kinds of behavior are clear. (The parameters of the circulation patterns shown in Fig. 2 are marked by circles in Fig. 3.) for large L, for example, $L = O$(100–1000 km), R/S increases as L decreases, ranging from $R/S < 3$ for $L \approx 2000$ km to a maximum of $R/S \approx 30$ for $L \approx 100$ km. When the meridional scale of the sink is reduced further, R/S *decreases* with L, that is, it appears that $R/S \to 0$ when $L \to 0$. The dividing line between this reversal of behavior as a function of L is shown by the dashed line in Fig. 3 and is governed by $B = 1$ with R/S being inversely related to L when $B < 1$ and R/S behaving in the same sense as L when $B > 1$.

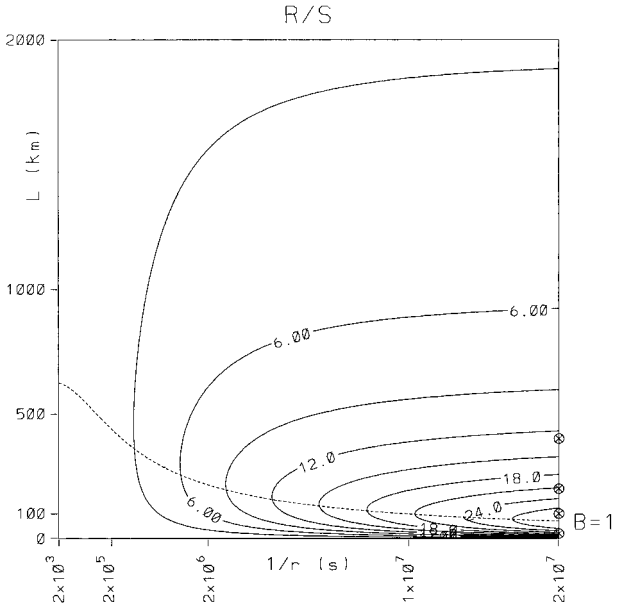

FIG. 3. The ratio of maximum recirculation strength to that of upwelling, R/S (contour interval: 3), as a function of the bottom friction coefficient, r, and meridional scale of the sink, L, for $\theta_0 = 30°$N and $x_0 = 200$ km. The circles along the right vertical axis mark the parameters of the circulation patterns shown in Fig. 2. The dashed line corresponds to $B = 1$ ($B > 1$ below this line and $B < 1$ above this line).

The sensitivity of R/S to the remaining important physical parameter, x_0, is as follows (not shown): as x_0 decreases, R/S increases, and the critical line $B = 1$ moves toward smaller L. This indicates, physically, that when the sink is zonally localized near the eastern boundary, the resulting recirculating flow strength is higher than the case in which the sink is distributed over a larger zonal distance from the eastern boundary.

The inviscid solution is obtained when $r \to 0$ and for $B < 1$, $d \to +\infty$. Hence, $\exp[\ln(B)/(1 - B)] \to 0$ and $\exp[B\ln(B)/(1 - B)] \to 1$. Therefore, from (43),

$$\left(\frac{R}{S}\right)_0 = \lim_{r \to 0}\frac{R}{S} \to \frac{\pi}{2}\frac{f_0}{\beta L}. \tag{44}$$

This result is in approximate agreement with $(R/S)_0 = f_0/\beta L$ resulting from the scaling analysis of inviscid equations (Pedlosky 1996; Spall 2000). The proportionality factor, $\pi/2$, appears to be the ''shape factor'' due to forcing function.

Normalizing R/S in (43) by the inviscid solution (44), we get

$$\frac{(R/S)}{(R/S)_0} = \frac{d}{(1 + d + B)}\frac{1}{(1 - B)} \times \left\{\exp\left(\frac{\ln B}{1 - B}\right) - \exp\left(B\frac{\ln B}{1 - B}\right)\right\}. \tag{45}$$

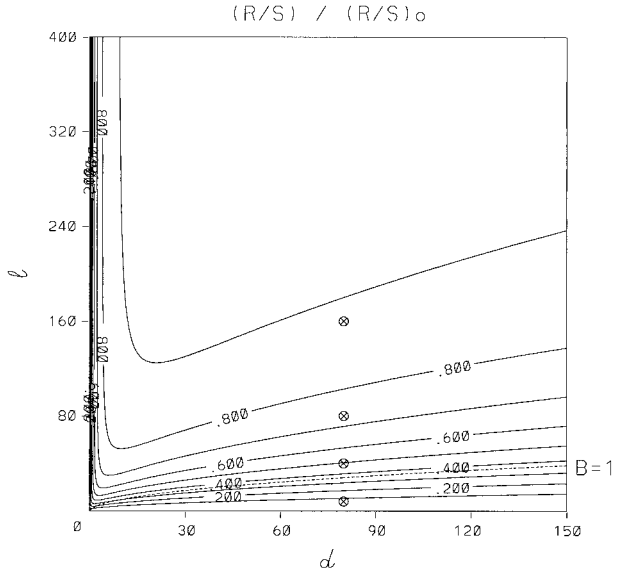

FIG. 4. Normalized ratio of maximum recirculation strength to that of upwelling, $(R/S)/(R/S)_0$ as a function of d and l (contour interval: 0.1) for the bottom dissipation case. The circles mark the parameters of the circulation patterns shown in Fig. 2 ($d = 80$, $l = 160$, 80, 40, 8). The dashed line corresponds to $B = 1$.

The rhs of (45), when different from unity, quantifies the effect of friction on the recirculating flow. The quantity $(R/S)/(R/S)_0$ is plotted as a function of nondimensional parameters d and l in Fig. 4, which illustrates the behavior of the β-plume system in the entire parameter space. First, we note that when $d < O(1)$, $(R/S)/(R/S)_0 \to 0$. This regime corresponds to the case when the sink is zonally localized very close to the eastern boundary and is damped by friction. This is the case considered in detail by Spall (2000). Outside of this regime [$d \gg O(1)$], when $l \to \infty$, $(R/S)/(R/S)_0 \to 1$; hence the frictional effects are small and the inviscid solution is recovered. For small l, friction becomes important and $(R/S)/(R/S)_0 < 1$. As $l \to 0$, the recirculation diminishes, particularly after crossing the $B = 1$ line (shown by dashed line; parameters of the circulation patterns shown in Fig. 2 are also marked). This is the new regime introduced in the present study.

The limiting behavior of $(R/S)/(R/S)_0$ for $d \to 0$ and $l \to 0$ is formally shown by rewriting (45) as

$$\frac{(R/S)}{(R/S)_0} = \frac{dl^2}{(dl^2 + l^2 - \pi^2 d^2)} \times \left\{ \exp\left(\frac{\ln B}{1 - B}\right) - \exp\left(B \frac{\ln B}{1 - B}\right) \right\}, \quad (46)$$

and considering the trajectory $l = md$ on the (d, l) plane, with $m > 0$. Substitution yields

$$\frac{(R/S)}{(R/S)_0} = \frac{m^2 d^3}{(m^2 d^3 + m^2 d^2 - \pi^2 d^2)} \times \left\{ \exp\left(\frac{\ln \tilde{B}}{1 - \tilde{B}}\right) - \exp\left(\tilde{B} \frac{\ln \tilde{B}}{1 - \tilde{B}}\right) \right\}, \quad (47)$$

where $\tilde{B} = \sqrt{(d/2)^2 + (\pi/m)^2} - d/2$.

First, we consider the case with $m \neq \pi$. In this case

$$\lim_{d \to 0} \frac{m^2 d}{(m^2 d + m^2 - \pi^2)} = 0 \quad \text{and} \quad \lim_{d \to 0} \tilde{B} = \frac{\pi}{m}.$$

Hence, on the whole,

$$\lim_{d \to 0} \frac{R/S}{(R/S)_0} = 0. \quad (48)$$

In the case with $m = \pi$,

$$\lim_{d \to 0} \frac{m^2 d^3}{(m^2 d^3 + m^2 d^2 - m^2 d^2)} = 1 \quad \text{and} \quad \lim_{d \to 0} \tilde{B} = 1,$$

and after a few manipulations

$$\lim_{d \to 0} \left\{ \exp\left(\frac{\ln \tilde{B}}{1 - \tilde{B}}\right) - \exp\left(\tilde{B} \frac{\ln \tilde{B}}{1 - \tilde{B}}\right) \right\} = 0,$$

and therefore we arrive again at (48).

The upward sloping of $(R/S)/(R/S)_0$ contours for high values of d (Fig. 4) is due to the fact that the sink becomes distributed over a large zonal distance (rather than becoming gradually more distant from the eastern boundary), and therefore the recirculation intensity decreases for a fixed l. It is a consequence of the sink function (2).

Finally, $(R/S)/(R/S)_0$ is plotted for the lateral dissipation solutions as well, as a function of nondimensional parameters d^* and l^* in Fig. 5. Figure 5a shows $(R/S)/(R/S)_0$ contours based on the solution given in (27). As discussed before, this solution has singularity when (28) is satisfied, while the behavior elsewhere is qualitatively similar to that from the bottom dissipation case. Figure 5b shows $(R/S)/(R/S)_0$ contours from the solution given in (35), which remains finite where (27) has singularity.

c. Westward penetration distance

An interesting feature of the β-plume solutions shown in Fig. 2 is their westward penetration distance. The β plumes in Figs. 2a, b clearly extend far beyond the zonal extent of the domain shown here (2000 km), whereas the one in Fig. 2c has approximately the same extent as the domain and that in Fig. 2d extends only few hundred kilometers westward. To investigate this issue, we define the westward penetration distance of the β plume as the distance from the eastern boundary along $y = 1/2$ at which the strength of the recirculating transport becomes negligible with respect to the maximum transport, that is,

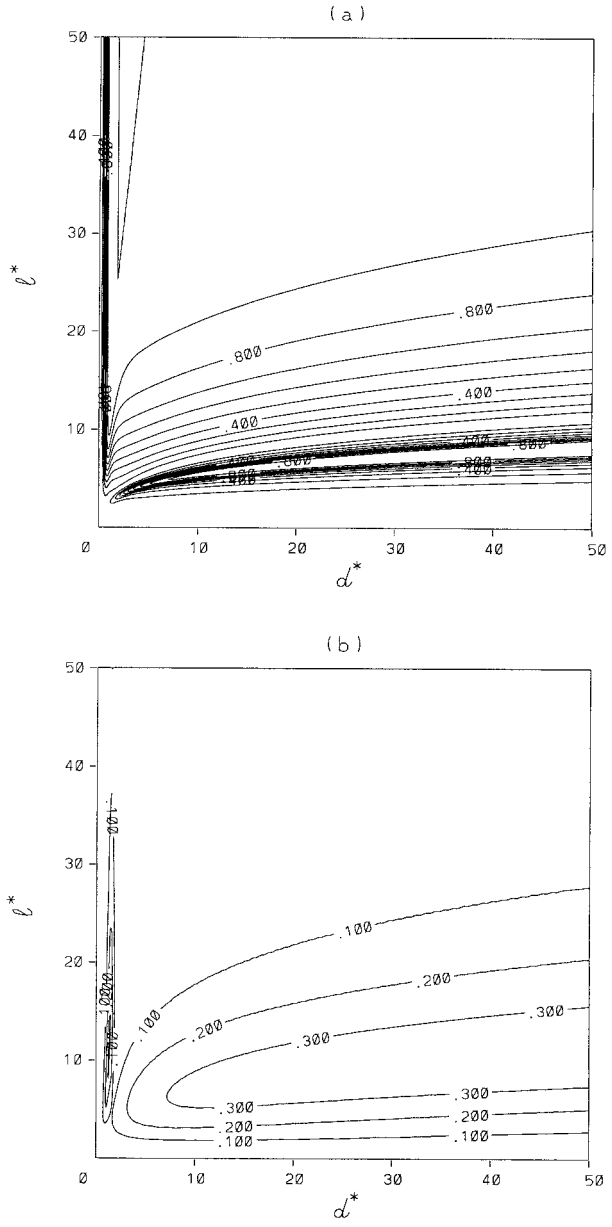

FIG. 5. Normalized ratio of maximum recirculation strength to that of upwelling, $(R/S)/(R/S)_0$ as a function of d^* and l^* for the lateral dissipation case (a) from solution (27) and (b) from solution (35) (contour interval: 0.1).

$$\frac{\psi\left(x_p, \frac{1}{2}\right)}{\psi\left(x_{\max}, \frac{1}{2}\right)} = \varepsilon, \tag{49}$$

where x_p is the westward penetration distance and ε is a small value.

We find that (49) is difficult to solve analytically, and therefore (49) is solved numerically for x_p. Figure 6

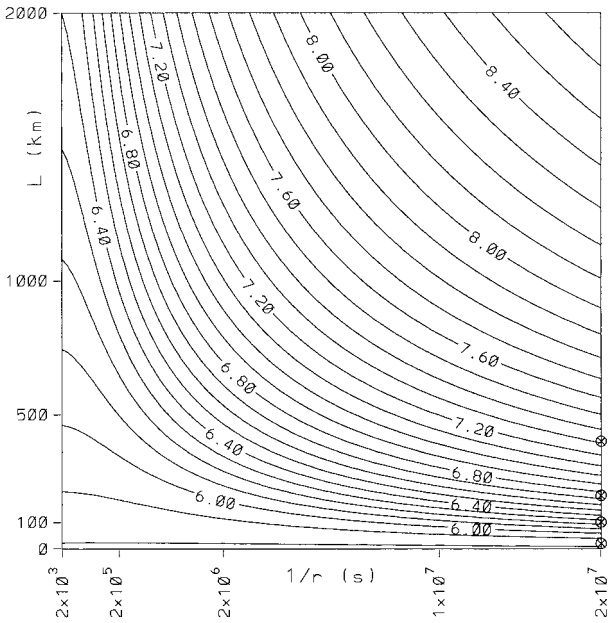

FIG. 6. Log of westward penetration distance, $\log_{10}(-x_p')$, where $x_p' = x_p L$ is in meters, as a function of the bottom friction coefficient, r, and meridional scale of the sink, L, for $\theta_0 = 30°$N and $x_0 = 200$ km (contour interval: 0.1). The circles mark parameters of the circulation patterns shown in Fig. 2.

shows $\log_{10}(-x_p')$, where $x_p' = x_p L$ is in meters, as a function of L and r for $x_0 = 200$ km and $\theta_0 = 30°$N (i.e., as in Fig. 2). The sensitivity parameter is taken as $\varepsilon = 0.05$ (i.e., 20 contour lines) to be able to make a direct comparison to Fig. 2. Obviously, westward penetration distance becomes higher for smaller values of ε; however, our objective is to gain insight into the qualitative behavior of x_p. Figure 6 indicates, quite intuitively, that westward penetration distance decreases (increases) as the meridional sink scale L decreases (increases) and as the bottom friction coefficient r increases (decreases). For the parameters of the circulation patterns shown in Figs. 2a–d, $x_p' \approx -10^{7.3}$ m $\approx -20\,000$ km for $r = 5 \times 10^{-8}$ s^{-1} and $L = 400$ km, $x_p' \approx -10^{6.75}$ m ≈ -5600 km for $L = 200$ km, $x_p' \approx -10^{6.25}$ m ≈ -1800 km for $L = 100$ km, and $x_p' \approx -10^{5.85}$ m ≈ -700 km for $L = 50$ km.

Finally, another quantity of interest, $x_{\max}$, the distance from the eastern boundary at which the maximum recirculating transport is reached, is plotted from (41). Figure 7a illustrates dimensional $x_{\max}' = x_{\max} L$ plotted as a function of L and r (and for selected parameters, $x_0 = 200$ km and $\theta_0 = 30°$N, as before) and indicates that the maximum recirculation point $x_{\max}'$ moves closer to the eastern boundary as the meridional sink scale L decreases and as the bottom friction coefficient r increases. For the parameters of the circulation patterns shown in Figs. 2a–d, $x_{\max}' \approx -715$, -475, -275, and -50 km, respectively. (The resemblance between Fig. 7a and Fig. 6 seems to imply a simple relation between

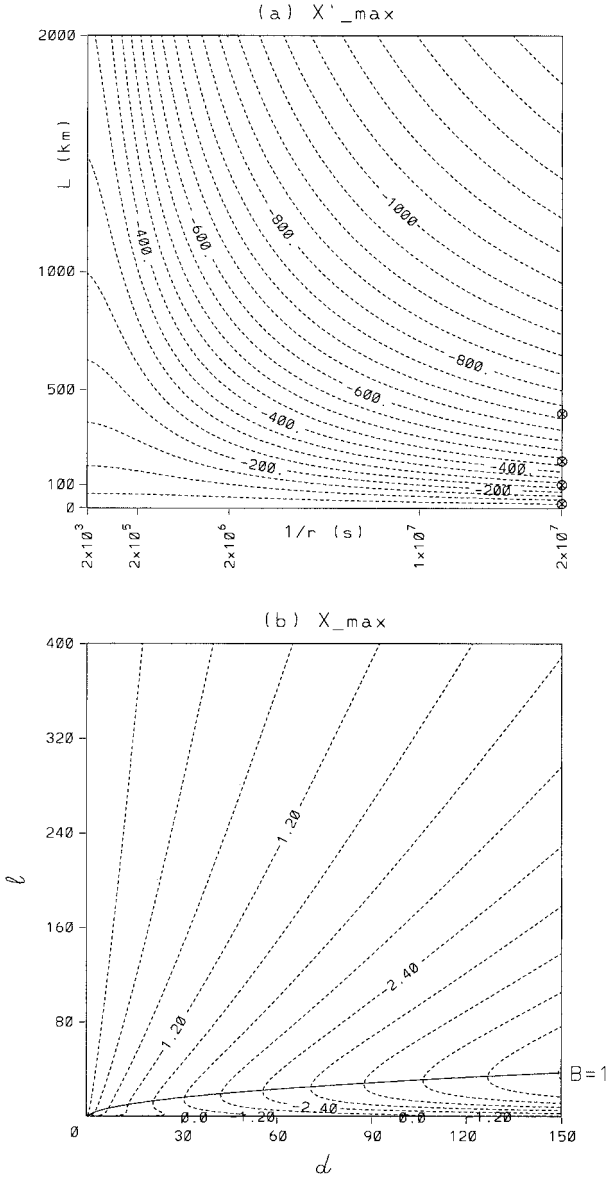

FIG. 7. The location of the maximum recirculating transport. (a) Dimensional $x'_{max} = x_{max}L$ (contour interval: 50 km) as a function of the bottom friction coefficient, r, and meridional scale of the sink, L, for $\theta_0 = 30°$N and $x_0 = 200$ km. The circles mark parameters of the circulation patterns shown in Fig. 2. (b) Nondimensional x_{max} (contour interval: 0.3) as a function of d and l. The solid line marks $B = 1$.

x'_{max} and x'_p.) Finally, x_{max} is plotted also in nondimensional (d, l) space in Fig. 7b, which indicates that $x_{max} \to 0$, as $d \to 0$ and also as $l \to 0$, after crossing the $B = 1$ line. The plots for x_{max} and x_p for the lateral dissipation case are qualitatively similar to those shown for the bottom dissipation case.

4. Stability analysis

The bidirectional jets forming the β plume are likely to be unstable due to strong shears when the meridional extent of the forcing becomes small. In this section, we conduct a stability analysis to determine the parameter regime, in which the β plumes are candidates for instability.

We consider flows far away from the region of potential vorticity forcing under the assumption that x_0 is sufficiently small, and therefore the following ''asymptotic'' solutions apply for $x \ll 0$.

For the bottom dissipation case, the solution far from the source is approximated by

$$\psi \approx \psi_{bf} \propto \sin(\pi y) \exp\left[\left(-\frac{l}{2} + \sqrt{\left(\frac{l}{2}\right)^2 + \pi^2}\right)x\right], \quad (50)$$

and for the lateral dissipation case, the asymptotic solution becomes

$$\psi \approx \psi_{lf} \propto \sin(\pi y) \exp\left[\left(\pi + \frac{\epsilon}{2} - \sqrt{\pi\epsilon + \left(\frac{\epsilon}{2}\right)^2}\right)x\right]. \quad (51)$$

Note that the quantity within parentheses in (51) is λ_- from (20). We also point out that the dynamic boundary conditions (no-slip or free-slip) are not important away from the boundary, hence not in the above asymptotic solution.

The common feature of the asymptotic solutions (50) and (51) is that

$$\nabla^2\psi = -\alpha^2\psi \quad (52)$$

for suitable values of α. That is to say, from (50), we have

$$\nabla^2\psi_{bf} = l\left[\frac{l}{2} - \sqrt{\left(\frac{l}{2}\right)^2 + \pi^2}\right]\psi_{bf}, \quad (53)$$

while from (51) we have

$$\nabla^2\psi_{lf} = 2\sqrt{\pi\epsilon + \frac{\epsilon^2}{4}}\left[\sqrt{\pi\epsilon + \frac{\epsilon^2}{4}} - \left(\pi + \frac{\epsilon}{2}\right)\right]\psi_{lf}. \quad (54)$$

The terms inside the square brackets appearing in (53) and (54) are *identically negative*, such that the relative vorticity is negatively correlated with the corresponding streamfunction in both asymptotic solutions. Note that (52) trivially gives

$$\frac{\partial\nabla^2\psi}{\partial\psi} < 0, \quad (55)$$

which is an immediate consequence of (53) and (54). The inequality (55) naturally leads us to resort to the instability theory developed by Pedlosky (1987). In order to apply this instability theory, a scaling analysis of the governing equations is needed to determine whether (52) is satisfied to some lowest-order approximation. To this end, we consider the following steady equations, which now include the inertial terms:

$$J(\psi', \nabla^2\psi') + \beta\frac{\partial\psi'}{\partial x} = \frac{f_0}{H}w' - r\nabla^2\psi' \quad \text{or} \quad (56)$$

$$J(\psi', \nabla^2\psi') + \beta\frac{\partial\psi'}{\partial x} = \frac{f_0}{H}w' + \nu\nabla^4\psi'. \quad (57)$$

Equations (56) and (57) are nonlinear versions of (1). Introducing the nondimensional variables defined in (4), we get

$$J(\psi, \nabla^2\psi) = \frac{\beta^2L^2H}{f_0W}\left(w - \frac{\partial\psi}{\partial x} - \frac{\delta_s}{L}\nabla^2\psi\right) \quad \text{or} \quad (58)$$

$$J(\psi, \nabla^2\psi) = \frac{\beta^2L^2H}{f_0W}\left[w - \frac{\partial\psi}{\partial x} + \left(\frac{\delta_M}{L}\right)^3\nabla^4\psi\right]. \quad (59)$$

We point out that both the lhs (Jacobian) and the rhs of (58) and (59) are satisfied separately by the asymptotic solutions (50) and (51). Therefore, (50) and (51) satisfy the entire equations (58) and (59), respectively. The necessary conditions for instability, that is, for (55) to hold, are

$$\frac{\beta^2L^2H}{f_0W} \ll 1 \quad \text{and} \quad \frac{\delta_s}{L} \ll 1 \quad \text{or} \quad \left(\frac{\delta_M}{L}\right)^3 \ll 1. \quad (60)$$

If inequalities (60) are fulfilled, the leading vorticity equation is simply $J(\psi, \nabla^2\psi) = 0$, where ψ satisfies (52). Thus, ψ is candidate to instability. The inequality $\beta^2L^2H/f_0W \ll 1$ implies $\beta y_* \ll \zeta_*$, and hence a marked meridional gradient of relative vorticity, associated with the sinusoidal form of ψ [see (50) and (51)], which favors barotropic instability. Moreover, inequalities $\delta_s/L \ll 1$ and $(\delta_M/L)^3 \ll 1$ indicate that dissipation is sufficiently weak to make the damping timescale too short to control the growth rate of the perturbation.

In order to give an example, we seek to determine L and friction coefficients r and ν, for which β plumes can become unstable. Using (37), the conditions (60) can be rewritten as

$$L \ll \left[\frac{\pi f_0 S}{2\beta^2 x_0 H}\right]^{1/3} \quad \text{and} \quad r \ll \left[\frac{\pi f_0 S\beta}{2x_0 H}\right]^{1/3} \quad \text{or}$$

$$\nu \ll \frac{\pi f_0 S}{2\beta x_0 H}. \quad (61)$$

Substituting $f_0 = 7.3 \times 10^{-5}$ s^{-1}, $\beta = 2 \times 10^{-11}$ m^{-1} s^{-1} and $x_0 = 200$ km, and taking reasonable values for $S = 1$ Sv and $H = 1000$ m, the conditions necessary for instability become in this case

$$L \ll 100 \text{ km} \quad \text{and} \quad r \ll 2 \times 10^{-6} \text{ s}^{-1} \quad \text{or}$$

$$\nu \ll 3 \times 10^4 \text{ m}^2 \text{ s}^{-1}. \quad (62)$$

5. Discussion and conclusions

In light of recent evidence that the entrainment of Atlantic water into the Mediterranean overflow may lead to the formation of the Azores Current and the Azores Countercurrent (Jia 2000; Özgökmen et al. 2001), the dynamics of β plumes driven by a sink of mass located at the eastern boundary of an ocean basin are investigated. The study is conducted by solving analytically the simplest possible governing equation of oceanic flow, the equivalent-barotropic, linear, steady quasigeostrophic equation, in which the sink of mass is represented by a source of potential vorticity, an approach that is justified based on the numerical experiments by Özgökmen et al. (2001). The objective of this study is to quantify the parameter regime in which friction becomes an important factor in the dynamics of β plumes. The present effort can be considered as a natural extension of the study by Spall (2000), in which the impact of friction on the β plumes was investigated using one-dimensional analytical solutions of quasigeostrophic equation and numerical experiments. The quasigeostrophic solutions in Spall (2000) compared well with the primitive equation numerical model solutions, lending credibility to the use of quasigeostrophic dynamics to describe the boundary layer structure.

By scaling the ratio of the strength of the recirculation and the strength of the sink (R/S), by that from the inviscid solution $(R/S)_0$, the regimes are identified in which friction becomes a dominant factor: $(R/S)/(R/S)_0$ is plotted as a function of d and l, the zonal and meridional scales of the sink, divided by the frictional boundary layer scale. It is confirmed that friction becomes an important factor and reduces the strength of the recirculating flow when $d < O(1)$, as found by Spall (2000). The primary new finding of this study is that the recirculating flow component disappears due to frictional effects also when the meridional extent of the sink becomes small. However, unlike for the zonal extent of the sink, which affects the recirculating component only if it is on the order of the frictional boundary layer scale, the deviation of the recirculating flow strength from that given by the inviscid solution is apparent for meridional sink scales, which are much larger than the frictional boundary layer scale, or for $l = O(10)$. We also quantify the location of the maximum recirculation and westward penetration distance of the plumes in the parameter space. A stability analysis is conducted to determine the parameter regime in which the β plumes are candidates for instability.

Finally, we outline the various simplifications in the system considered in this study and recommendations for future studies. First, separation of variables (6) does not permit meridional widening of β plumes toward the west. Second, only steady solutions are considered in the present study, and the model can be extended to incorporate time-varying behavior due to fluctuations in the forcing. The third and probably most important factor that needs to be addressed via numerical simulations is the effect of nonlinear inertial terms. Some of the other important factors, such as the effects of stratification and bottom topography on β plumes, have been

investigated in detail by Spall (2001) using a two-layer, planetary geostrophic model with a sloping bottom. One of the findings of Spall (2001) relevant to the present study and to that by Özgökmen et al. (2001) is that the upper-layer flow is not very sensitive to the presence of topography, but the deep β plume is eliminated.

Acknowledgments. T. M. Özgökmen greatly appreciates the support of the National Science Foundation Grant OCE 9711186 and the Office of Naval Research Grant N00014-01-1-0023. F. Crisciani acknowledges partial support from the Italian Space Agency (ASI). The authors thank Dr. C.G.H. Rooth for insightful comments on an earlier version of the manuscript. We thank M. Spall and the reviewers for extremely useful comments and criticism, which led to a major improvement of the manuscript.

REFERENCES

Baringer, M. O., and J. F. Price, 1997a: Mixing and spreading of the Mediterranean outflow. *J. Phys. Oceanogr.*, **27,** 1654–1677.

——, and ——, 1997b: Momentum and energy balance of the Mediterranean outflow. *J. Phys. Oceanogr.*, **27,** 1678–1692.

Cromwell, D., P. F. Challenor, and A. L. New, 1996: Persistent westward flow in the Azores Current as seen from altimetry and hydrography. *J. Geophys. Res.*, **101,** 11 923–11 933.

Gould, W. J., 1985: Physical oceanography of the Azores Front. *Progress in Oceanography*, Vol. 14, Pergamon, 167–190.

Iorga, M. C., and M. S. Lozier, 1999a: Signatures of the Mediterranean outflow from a North Atlantic climatology 1. Salinity and density fields. *J. Geophys. Res.*, **104,** 25 985–26 009.

——, and ——, 1999b: Signatures of the Mediterranean outflow from a North Atlantic climatology 2. Diagnostic velocity fields. *J. Geophys. Res.*, **104,** 26 011–26 029.

Jia, Y., 2000: Formation of an Azores Current due to Mediterranean overflow in a modeling study of the North Atlantic. *J. Phys. Oceanogr.*, **30,** 2342–2358.

Käse, R. H., and G. Siedler, 1982: Meandering of the subtropical front south-east of the Azores. *Nature*, **300,** 245–246.

——, and W. Krauss, 1996: The Gulf Stream, the North Atlantic Current, and the origin of the Azores Current. *The Warmwatersphere of the North Atlantic Ocean*, W. Krauss, Ed., Gebrüder Borntraeger, 291–331.

——, W. Zenk, T. B. Sanford, and W. Hiller, 1985: Currents, fronts and eddy fluxes in the Canary Basin. *Progress in Oceanography*, Vol. 14, Pergamon, 231–257.

Klein, B., and G. Siedler, 1989: On the origin of the Azores Current. *J. Geophys. Res.*, **94,** 6159–6168.

Mauritzen, C., Y. Morel, and J. Paillet, 2001: On the influence of Mediterranean Water on the Central Waters of the North Atlantic Ocean. *Deep-Sea Res. I*, **48,** 347–381.

Onken, R., 1993: The Azores Countercurrent. *J. Phys. Oceanogr.*, **23,** 1638–1646.

Özgökmen, T. M., E. P. Chassignet, and C. G. H. Rooth, 2001: On the connection between the Mediterranean outflow and the Azores Current. *J. Phys. Oceanogr.*, **31,** 461–480.

Pedlosky, J., 1987: *Geophysical Fluid Dynamics.* Springer, 617–623.

——, 1996: *Ocean Circulation Theory.* Springer, 405–408.

Spall, M., 2000: Buoyancy-forced circulations around islands and ridges. *J. Mar. Res.*, **58,** 957–982.

——, 2001: Large-scale circulations forced by localized mixing over a sloping bottom. *J. Phys. Oceanogr.*, **31,** 2369–2384.

Spiegel, M. R., 1991: *Mathematical Handbook of Formulas and Tables.* McGraw-Hill, 105 pp.

Stommel, H., 1982: Is the South Pacific helium plume dynamically active? *Earth Planet. Sci. Lett.*, **61,** 63–67.